

The Phase Structure of the Gross-Neveu Model with Thirring Interaction at the Next to Leading Order of $1/N$ Expansion

Takashi Dateki¹

Department of Physics, Nagoya University

Nagoya 464-01, Japan

Abstract

We study the critical behavior of the D ($2 < D < 4$) dimensional Gross-Neveu model with a Thirring interaction, where a vector-vector type four-fermi interaction is on equal terms with a scalar-scalar type one.

By using inversion method up to the next-to-leading order of $1/N$ expansion, we construct a gauge invariant effective potential. We show the existence of the chiral order phase transition, and determine explicitly the critical surface. It is observed that the critical behavior is mainly controlled by the Gross-Neveu coupling g . The critical surface can be divided into two parts by the surface $g = 1$ which is the critical coupling in the Gross-Neveu model at the $1/N$ next-to-leading order, and the form of the critical surface is drastically change at $g = 1$. Comparison with the Schwinger-Dyson(SD) equation is also discussed. Our result is almost the same as that derived in the SD equation. Especially, in the case of pure Gross-Neveu model, we succeed in deriving exactly the same critical line as the one derived in the SD equation.

1 Introduction

One of the most important subject in the elementary particle physics is how to treat non-perturbative effect and how to obtain non-perturbative information. Since the work of Nambu-Jona-Lasinio(NJL)[1], chiral symmetry breaking have been studied extensively in various models, e.g. QCD, strong coupling QED[2], gauged NJL[3, 4], etc.. Particularly, the mechanism of dynamical mass generation has been applied to models beyond the

¹e-mail: dateki@eken.phys.nagoya-u.ac.jp

standard model, for example, walking technicolor[5], top mode standard model[6], etc.. In these models, scalar 4-fermion interaction plays an important role. Such a 4-fermion interaction in $D(2 < D < 4)$ dimensions, the Gross-Neveu model[7], has been extensively studied.

Recently dynamical symmetry breaking and dynamical mass generation in the Thirring model[8], which has vector-vector type 4-fermion interaction in D dimensions($2 < D < 4$), has been studied by many authors [9, 10, 11]. Usually the Thirring model is studied in the form where the fermion has a minimal coupling with a massive vector boson through introduction of the vector auxiliary field. Although this theory (as well as original Thirring model) has no local gauge symmetry, several authors treated this massive gauge field as a genuine gauge field[9]. Itoh et al. [10] have reformulated Thirring model as a gauge theory by using the hidden local symmetry[12], and emphasized the advantage of maintaining such a manifest gauge symmetry in the analysis of Thirring model in terms of SD equation. Kondo[11] further analyzed such a formulation in terms of the inversion method[13].

It would be interesting to consider the critical behavior of the model in which the above two types of 4-fermi interaction coexist. Actually, Kim et al.[15] studied such a model but without manifest gauge symmetry. Due to each of the gauge symmetry their analysis of the SD equation unfortunately depends on their assumptions.

In this paper, we analyze Gross-Neveu model with Thirring interaction by introducing hidden local symmetry and using the inversion method[13] instead of SD equation. We obtained the generating functional of the next-to-leading order and the effective potential by the inversion method. The critical line is obtained in the parameter space (g, g_v, N) where g and g_v are the dimensionless couplings of Gross-Neveu and Thirring model, respectively, and N is the number of fermions. The phase structure drastically changes at $g=1$ which is the critical coupling of the pure Gross-Neveu model at the leading order of $1/N$ expansion. For $g > 1$ the phase structure is essentially determined by the Gross-Neveu interaction being only operative in the $1/N$ -subleading corrections, while for $g < 1$, the the symmetry breaking take place only due to the subleading effects where the Thirring interaction yields attractive force to form the condensate in contrast to the Gross-Neveu interaction which is opposite.

Following the procedure of Ref.[10], we reformulate the original theory as a gauge theory in section 2. In section 5 and section 6, we calculate the effective potential for the chiral order parameter $\langle\bar{\psi}\psi\rangle$, by using the inversion method in $1/N$ expansion. Based on this potential, we study spontaneous chiral symmetry breaking and explicitly obtain the critical surface which is the boundary between symmetric phase and spontaneously broken phase. Comparison with the SD equation is discussed in section 7.

2 Hidden Local Symmetry

Let us consider D -dimensional Gross-Neveu model with Thirring interaction ($2 < D < 4$). The Lagrangian is given by

$$\tilde{\mathcal{L}} = \bar{\Psi}(x)i\partial\Psi(x) + \frac{G_S}{2N}(\bar{\Psi}(x)\Psi(x))^2 - \frac{G_V}{2N}(\bar{\Psi}(x)\gamma^\mu\Psi(x))^2 + J\bar{\Psi}(x)\Psi(x), \quad (1)$$

where Ψ^a is a 4-component Dirac spinor with index a ($a = 1, 2, \dots, N$) and belongs to a fundamental representation of $U(N)$, and γ_μ ($\mu = 0, 1, 2, \dots, D-1$) are 4×4 matrices satisfying the Clifford algebra $\{\gamma_\mu, \gamma_\nu\} = 2g_{\mu\nu}\mathbf{1}$. Index a will be omitted in the following. Here we introduced the source $J = \text{constant}$ in order to study $\langle\bar{\Psi}\Psi\rangle$. Using the auxiliary field, we may rewrite this Lagrangian in to the form

$$\tilde{\mathcal{L}}' = \bar{\Psi}(i\partial + J)\Psi - \frac{1}{2G_S}\sigma^2 - \frac{1}{\sqrt{N}}\sigma\bar{\Psi}\Psi + \frac{1}{2G_V}\tilde{A}_\mu^2 + \frac{1}{\sqrt{N}}\bar{\Psi}\tilde{A}\Psi, \quad (2)$$

where the auxiliary massive vector field \tilde{A}_μ corresponding to the current $\bar{\Psi}\gamma_\mu\Psi$ is not really a gauge boson as it stands, and this Lagrangian actually has no gauge symmetry.

Itoh et al.[10] introduced hidden local symmetry to the Thirring model and treated it really as a gauge theory. Following the same procedure as in Ref.[10], we introduce hidden local symmetry to our model. What we should do is only the following substitution:

$$\begin{cases} \Psi = e^{-i\phi}\psi, \\ \tilde{A}_\mu = A_\mu - \sqrt{N}\partial_\mu\phi. \end{cases} \quad (3)$$

The Lagrangian(2) is written as

$$\tilde{\mathcal{L}}'' = \bar{\psi}(i\partial + J)\psi - \frac{1}{2G_S}\sigma^2 - \frac{1}{\sqrt{N}}\sigma\bar{\psi}\psi + \frac{1}{2G_V}(A_\mu - \sqrt{N}\partial_\mu\phi)^2 + \frac{1}{\sqrt{N}}\bar{\psi}A\psi, \quad (4)$$

where ϕ is the NG boson for $U(1)_{\text{local}}$ symmetry breaking, which is to be absorbed into the longitudinal mode of massless gauge boson A_μ . $\tilde{\mathcal{L}}''$ is gauge-equivalent to the Lagrangian $\tilde{\mathcal{L}}'$. Actually, if we take the unitary gauge ($\theta = -\phi$), the Lagrangian $\tilde{\mathcal{L}}''$ reduces to $\tilde{\mathcal{L}}'$. It is noted that in contrast to $\tilde{\mathcal{L}}'$ which has no gauge symmetry, $\tilde{\mathcal{L}}''$ has a $U(1)_{\text{local}}$ symmetry:

$$\begin{cases} A_\mu \longrightarrow A'_\mu = A_\mu + \sqrt{N}\partial_\mu\theta , \\ \psi \longrightarrow \psi' = e^{i\theta}\psi , \\ \phi \longrightarrow \phi' = \phi + \theta . \end{cases} \quad (5)$$

The total Lagrangian can be obtained by adding to (4) the gauge fixing term and Faddeev-Popov(FP) ghost term:

$$\mathcal{L}_{GF+FP} = -i\delta_B(\bar{c}f[A, c, \bar{c}, B, \phi]) , \quad (6)$$

and is invariant under the following BRS transformation:

$$\begin{aligned} \delta_B A_\mu(x) &= \partial_\mu c(x) , \\ \delta_B B(x) &= 0 , \\ \delta_B c(x) &= 0 , \\ \delta_B \bar{c}(x) &= iB(x) , \\ \delta_B \phi(x) &= \frac{1}{\sqrt{N}}c(x) , \\ \delta_B \psi(x) &= \frac{i}{\sqrt{N}}c(x)\psi(x) , \\ \delta_B \sigma(x) &= 0 , \end{aligned} \quad (7)$$

where $c(x), \bar{c}(x)$ are the FP ghost fields and $B(x)$ is the Nakanishi-Lautrap field. If we chose $f(A, c, \bar{c}, B, \phi) = F(A, \phi) + \frac{\xi}{2}B$, FP ghost is decoupled from the system. By integrating out B , we can rewrite gauge fixing term \mathcal{L}_{GF} as

$$\mathcal{L}_{GF} = -\frac{1}{2\xi}F(A, \phi)^2 . \quad (8)$$

Here, covariant gauge and R_ξ gauge corresponds to following choice for $F(A, \phi)$, respectively.

$$F(A, \phi) = \partial^\mu A_\mu : \text{covariant gauge} , \quad (9)$$

$$F(A, \phi) = \partial^\mu A_\mu + \frac{\sqrt{N}}{G_V} \xi \phi : R_\xi \text{ gauge} . \quad (10)$$

In the covariant gauge(9), NG boson $\phi(x)$ is not decoupled except the Landau gauge($\xi = 0$). On the other hand, in the case of R_ξ gauge, $\phi(x)$ is completely decoupled from the system and therefore the system can easily be treated[10]. Here we choose R_ξ gauge. The total Lagrangian is obtained by adding \mathcal{L}_{GF} to the Lagrangian $\tilde{\mathcal{L}}''$:

$$\tilde{\mathcal{L}}''' = \mathcal{L} + \mathcal{L}_\phi , \quad (11)$$

$$\mathcal{L}_\phi = \frac{N}{G_V} \left\{ \frac{1}{2} (\partial\phi)^2 - \frac{\xi}{2G_V} \phi^2 \right\} , \quad (12)$$

$$\mathcal{L} = \bar{\psi}(i \not{\partial} + J)\psi + \frac{1}{\sqrt{N}} \bar{\psi} \not{A} \psi - \frac{1}{\sqrt{N}} \sigma \bar{\psi} \psi - \frac{1}{2G_S} \sigma^2 + \frac{1}{2G_V} A_\mu^2 - \frac{1}{2\xi} (\partial^\mu A_\mu)^2 , \quad (13)$$

$$\mathcal{L} = \bar{\psi}(i \not{\partial} + J)\psi + \frac{1}{2} \sigma i G_\sigma^{(0)-1} \sigma + \frac{1}{2} A^\mu i D_{\mu\nu}^{(0)-1} A^\nu + \frac{1}{\sqrt{N}} \bar{\psi} \not{A} \psi - \frac{1}{\sqrt{N}} \sigma \bar{\psi} \psi , \quad (14)$$

where $G_\sigma^{(0)}$ and $D_{\mu\nu}^{(0)}$ are the tree level scalar propagator and the tree level gauge boson propagator, respectively, which are written as

$$G_\sigma^{(0)} = \frac{i}{-G_S} , \quad (15)$$

$$D_{\mu\nu}^{(0)} = i \left\{ \frac{1}{G_V^{-1}} P_{\mu\nu}^T + \left(\frac{1}{G_V^{-1} + \xi^{-1} p^2} P_{\mu\nu}^L \right) \right\} , \quad (16)$$

$$P_{\mu\nu}^T \equiv g_{\mu\nu} - \frac{p_\mu p_\nu}{p^2} , \quad P_{\mu\nu}^L \equiv \frac{p_\mu p_\nu}{p^2} . \quad (17)$$

3 Vacuum Polarization

In this section, we calculate the vacuum polarization tensor in the Euclidean space. By making use of the gauge invariant Pauli-Villars regularization, it is shown that the 1-loop vacuum polarization tensor has the following form[14]:

$$\Pi_{\mu\nu}(p) = \Pi(p) P_{\mu\nu}^T , \quad (18)$$

where $\Pi(p)$ can be written as

$$\Pi(p) = \frac{-2(tr1)\Gamma(2 - D/2)}{(4\pi)^{D/2}} \int_0^1 dx \frac{(x - x^2)p^2}{\{J^2 + (x - x^2)p^2\}^{2-D/2}} \quad (19)$$

$$= -\frac{(tr1)\Gamma(2 - D/2)}{3(4\pi)^{D/2}} p^2 J^{D-4} F \left(2 - \frac{D}{2}, 2, \frac{5}{2}; -\frac{p^2}{4J^2} \right) , \quad (20)$$

with $F(\alpha, \beta, \gamma; z)$ being the hypergeometric function. Since the source J is infinitesimal, we can consider J as $2J/p \ll 1$ for non-zero momentum $p \neq 0$. Using the mathematical identity for the hypergeometric function,

$$F(\alpha, \beta, \gamma; z) = \frac{\Gamma(\gamma)\Gamma(\beta - \alpha)}{\Gamma(\beta)\Gamma(\gamma - \alpha)} (-z)^{-\alpha} F(\alpha, \alpha - \gamma + 1, \alpha - \beta + 1; z^{-1}) + \frac{\Gamma(\gamma)\Gamma(\alpha - \beta)}{\Gamma(\alpha)\Gamma(\gamma - \beta)} (-z)^{-\beta} F(\beta, \beta - \gamma + 1, \beta - \alpha + 1; z^{-1}), \quad (21)$$

we can expand $\Pi(p)$ in terms of $2J/p$:

$$\Pi(p) = f_0 p^{D-2} + f_2 p^{D-4} J^2 + f_D p^{-2} J^D + f_4 p^{D-6} J^4 + O(J^6, J^{D+2}), \quad (22)$$

$$f_0 = \frac{-2(tr1)\Gamma(2 - D/2)}{(4\pi)^{D/2}} B(D/2, D/2), \quad (23)$$

$$f_2 = -\frac{2(4 - D)(D - 1)}{(D - 2)} f_0, \quad (24)$$

$$f_4 = -\frac{2(6 - D)(D - 3)(D - 1)}{(D - 2)} f_0, \quad (25)$$

$$f_D = \frac{2^3 f_0}{D(D - 2)B(D/2, D/2)}. \quad (26)$$

Doing almost the same calculation as the one in $\Pi_{\mu\nu}(p)$, the 1-loop vacuum polarization for scalar propagator $\Pi_\sigma(p)$ is obtained as

$$\Pi_\sigma(p) = -c_0 + c_1 \int_0^1 dx \{J^2 + (x - x^2)p^2\}^{D/2-1}, \quad (27)$$

where c_0 and c_1 are defined by

$$c_0 = \frac{2(tr1)\Lambda^{D-2}}{(4\pi)^{D/2}\Gamma(D/2)(D - 2)}, \quad c_1 = \frac{2(tr1)\Gamma(2 - D/2)(D - 1)}{(4\pi)^{D/2}(D - 2)}. \quad (28)$$

For $p = 0$,

$$\Pi_\sigma(0) = -c_0 + c_1 J^{D-2}. \quad (29)$$

For $p \neq 0$, Π_σ can be expanded under the condition $2J/p \ll 1$:

$$\Pi_\sigma(p) = -c_0 + h_0 p^{D-2} + h_2 p^{D-4} J^2 + h_D p^{-2} J^D + h_4 p^{D-6} J^4, \quad (30)$$

$$h_0 = \frac{(tr1)\Gamma(D/2)\Gamma(2-D/2)(D-1)}{(4\pi)^{D/2}2^{D-2}(D-2)}, \quad (31)$$

$$h_2 = 2(D-1)h_0, \quad (32)$$

$$h_4 = 2(D-3)(D-1)h_0, \quad (33)$$

$$h_D = -\frac{(tr1)\Gamma(2-D/2)\Gamma(D/2)(D-1)}{(4\pi)^{D/2}\Gamma(D)D2^{1-D}(D-2)}. \quad (34)$$

When $2J/p > 1$, $\Pi_\sigma(p)$ should be expanded in terms of $p/2J$. However it has already been shown in the Thirring model that the contribution from the region $2J/p > 1$ is sufficiently small and therefore does not affect their conclusion [11]. Since essentially the same analysis can be applied to our case, we use (30) as long as $p \neq 0$.

4 Generating Functional

The generating functional $W[J]$ is given by

$$e^{iW[J]} = \int \mathcal{D}\psi \mathcal{D}\bar{\psi} \mathcal{D}\sigma \mathcal{D}A e^{iS}. \quad (35)$$

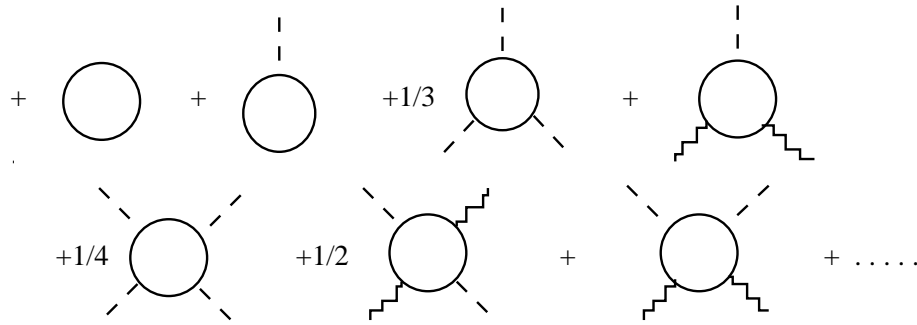
First we integrate out the fermion fields:

$$e^{iW[J]} = \int \mathcal{D}\sigma \mathcal{D}A \text{Det} \left\{ i \not{\partial} - \frac{1}{\sqrt{N}} \sigma + \frac{1}{\sqrt{N}} \not{A} \right\} \\ \times \exp \left\{ \frac{1}{2} \sigma i G_\sigma^{(0)-1} \sigma + \frac{1}{2} A^\mu i D_{\mu\nu}^{(0)-1} A^\nu \right\} \quad (36)$$

$$\equiv \int \mathcal{D}\sigma \mathcal{D}A e^{iS_{eff}}. \quad (37)$$

S_{eff} is the effective action which includes fermion loop effects:

$$iS_{eff}[\sigma, A] \\ = i \left\{ \frac{1}{2} \sigma i G_\sigma^{-1} \sigma + \frac{1}{2} A^\mu i D_{\mu\nu}^{-1} A^\nu \right\}$$



(38)

where $G_\sigma(p)$ and $D_{\mu\nu}(p)$ are the scalar propagator the gauge propagator, respectively, at the leading order of the $1/N$ expansion:

$$iG_\sigma^{-1}(p) = iG_\sigma^{(0)-1}(p) - \Pi_\sigma(p) , \quad (39)$$

$$iD_{\mu\nu}^{-1}(p) = iD_{\mu\nu}^{(0)-1}(p) - \Pi_{\mu\nu}(p) . \quad (40)$$

After integrating out the fermion field, we have an infinite number of non-local vertices in eq.(38). $W[J]$ is given by calculating all vacuum graphs which are made by connecting these non-local vertices in the $1/N$ expansion.

First we restrict ourselves to the leading order of $1/N$ expansion, $O(N)$. Since the source J is infinitesimal, the higher order terms with respect to J can be omitted in the calculation of $W[J]$. We expand $W[J]$ with respect to J and we will omit the terms higher than J^D . Therefore we consider the order of various graphs in order to estimate which graphs should be included in $W[J]$ up to $O(J^D)$. For example, we estimate the graphs Fig.1-2 which are contained in the order parameter $(\varphi(J) = \langle \bar{\psi}\psi \rangle_J)$:

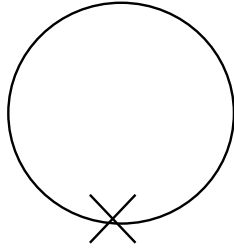


Fig.1

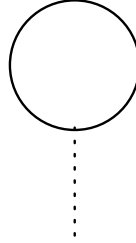


Fig.2

We have

$$\begin{aligned} \text{Fig.1} &= \langle \bar{\psi}\psi \rangle_{0J} = -iN \text{tr} \int_p \frac{i}{\not{p} + J} \\ &= Nc_0 J - \frac{Nc_1}{D-1} J^{D-1} . \end{aligned} \quad (41)$$

This graph is of order $O(J)$. From (41), we also note that $1/N$ leading tadpole diagram Fig.2 is of order $O(J)$.

Let us consider the n -point vertex shown in Fig.3 ($n \geq 3$). The case $n = 2$ in Fig.3 is the vacuum polarization and has already been absorbed into G_σ . This vertex is obtained by differentiating (41) with respect to source J :

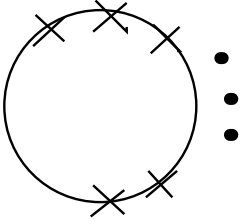


Fig.3

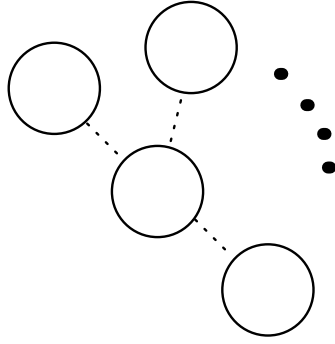


Fig.4

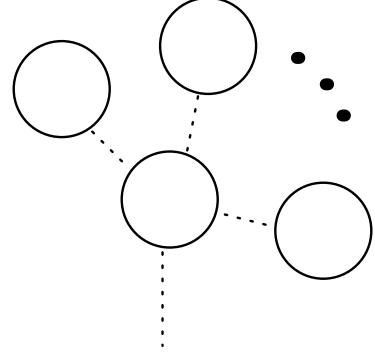


Fig.5

$$\begin{aligned} \text{Fig.3} &= \frac{1}{(n-1)!} \left(\frac{\partial}{i\partial J} \right)^{n-1} \left[Nc_0 J - \frac{Nc_1}{D-1} J^{D-1} \right] \\ &= \frac{-Nc_1(D-1)(D-2)\cdots(D-n+1)}{i^{n-1}(n-1)!(D-1)} J^{D-n} \end{aligned} \quad (42)$$

$$\sim O(J^{D-n}). \quad (43)$$

If $n > D$, (42) has negative power in J and diverges when $J = 0$. This is the consequence of existence of infrared divergence of Fig.3 in the case of $J = 0$. By using this vertex, we find that there exists a graph contributing to $W[J]$ at $O(J^D)$. Since Fig.4 includes Fig.3 ($O(J^{D-n})$) and n tadpoles ($O(J^n)$), Fig.4 becomes of order $O(J^D)$:

$$\text{Fig.4} \sim O(J^D). \quad (44)$$

It will be shown below that a graph which contains more than two non-local vertices of Fig.3 does not contribute to $W[J]$. It is clear that the tadpole diagram Fig.5 is of order $O(J^{D-1})$ with $D > 2$, and hence the order of this graph is higher than the simple tadpole Fig.2. Let us consider a graph which contains more than two vertices in Fig.3. There is at least one tadpole Fig.5. If we convert this tadpole Fig.5 into a simple tadpole Fig.2, the order of the graph becomes lower, and finally we can reduce the graph to Fig.4. Therefore we conclude that the order of such a graph as contains more than two vertices in Fig.3 is

higher than that of Fig.4 which is $O(J^D)$, and such a graph does not contribute to this order. We can easily find here all graphs Fig.6-8 contributing to $W[J]$ at $O(J^D)$ at the leading order of $1/N$ expansion:

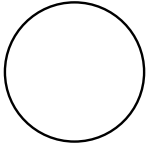


Fig.6

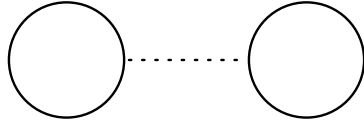


Fig.7

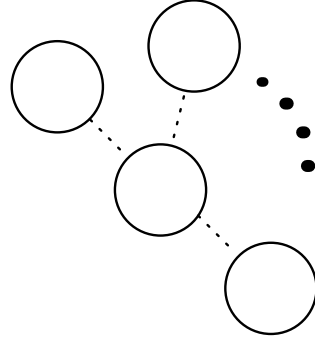


Fig.8

These graphs are easily calculated by using (41) and (42).

Similar arguments can be applied to the next-to-leading order of $1/N$ expansion. In the next-to-leading order, we have to consider the following non-local vertices in Fig.9-14 similar to Fig.3.

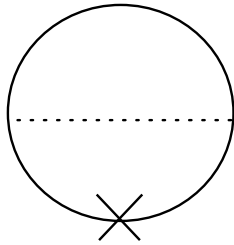


Fig.9

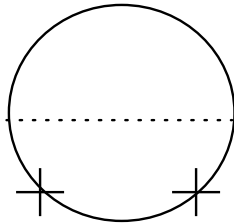


Fig.10

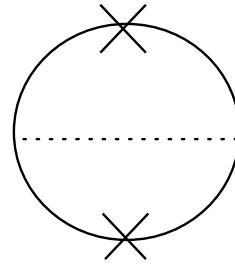


Fig.11

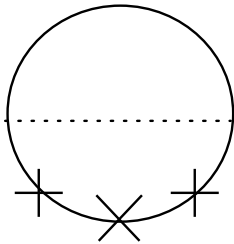


Fig.12

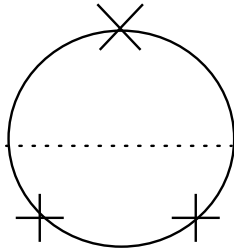


Fig.13

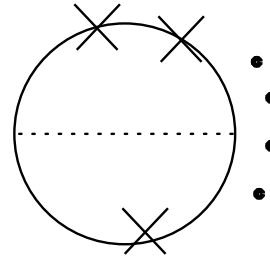


Fig.14

Fig.9 can be calculated by differentiating the scalar vacuum polarization (30).

$$\text{Fig.9} = \frac{1}{2} \text{Tr} \left[G_\sigma \frac{\partial}{i\partial J} (-i\Pi_\sigma) \right] \quad (45)$$

$$= \frac{-\Omega}{2} \int_p \left[iG_\sigma(p) \frac{\partial}{\partial J} \Pi_\sigma(p) \right] , \quad (46)$$

where Ω denotes the space-time volume, $\Omega = \int d^D x$. $G_\sigma(p)$ and $\Pi_\sigma(p)$ can be expanded in terms of J . Then Fig.9 is given by

$$\begin{aligned} \text{Fig.9} &= \frac{-1}{2} \int_p \frac{1}{G_S^{-1} - c_0 + h_0 p^{D-2}} \left\{ 1 - \frac{h_2 p^{D-4} J^2}{G_S^{-1} - c_0 + h_0 p^{D-2}} \right\} \\ &\quad \times \left\{ 2h_2 p^{D-4} J + D h_D p^{-2} J^{D-1} \right\} + O(J^{D+1}, J^3) , \end{aligned} \quad (47)$$

$$\equiv -B_1 J - B_2 J^{D-1} + O(J^3) , \quad (48)$$

$$\sim O(J) , \quad (49)$$

where

$$B_1 = \frac{4\alpha(D-1)\Lambda^{D-2}}{(D-2)} \left[1 - \frac{1}{\tilde{g}_s} \log(1 + \tilde{g}_s) \right] , \quad (50)$$

$$B_2 = \frac{\alpha D h_D}{(D-2)h_0} \log(1 + \tilde{g}_s) , \quad (51)$$

$$g = c_0 G_S , \quad \tilde{g}_s = \frac{h_0 \Lambda^{D-2}}{c_0} \left(\frac{g}{1-g} \right) , \quad \alpha = \frac{1}{(4\pi)^{D/2} \Gamma(D/2)} . \quad (52)$$

Fig.10,11,12,13, and generally $n(n > 3)$ -point vertex(Fig.14), can be obtained by the same procedure:

$$\text{Fig.10} + \frac{1}{2} \text{Fig.11} = \frac{1}{2 \cdot 2} \text{Tr} \left[G_\sigma \left(\frac{\partial}{i\partial J} \right)^2 (-i\Pi_\sigma) \right] \sim O(1) , \quad (53)$$

$$\text{Fig.12} + \text{Fig.13} = \frac{1}{2 \cdot 3!} \text{Tr} \left[G_\sigma \left(\frac{\partial}{i\partial J} \right)^3 (-i\Pi_\sigma) \right] \sim O(J^{D-3}) , \quad (54)$$

$$\text{Fig.14} = \frac{1}{2 \cdot n!} \text{Tr} \left[G_\sigma \left(\frac{\partial}{i\partial J} \right)^n (-i\Pi_\sigma) \right] \sim O(J^{D-n}) . \quad (55)$$

Thus $n(\geq 3)$ -point vertex Fig.14 as well as Fig.3 is of order $O(J^{D-n})$ and this fact leads to the same argument as at the leading order. Note that there appear several tadpoles($O(J)$) Fig.15-17 in the next-to-leading order:

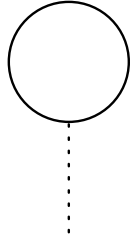


Fig.15

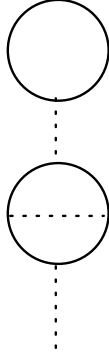


Fig.16



Fig.17

By using almost the same discussion as in the leading order, we find the following graphs will contribute to generating functional in the next-to-leading order. The above tadpoles Fig.15-17 and the following graphs Fig.18-24 can be easily calculated by use of (41), (49), (53) and (55).

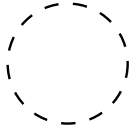


Fig.18

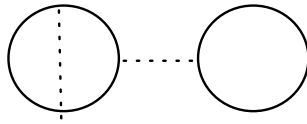


Fig.19

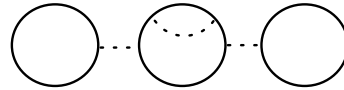


Fig.20

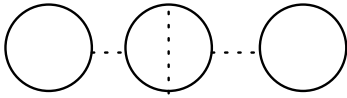


Fig.21

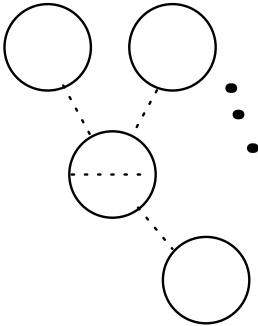


Fig.22

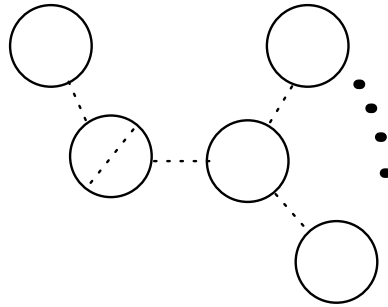


Fig.23

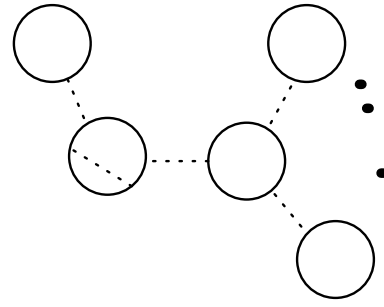


Fig.24

Now we include the gauge interaction, which can be performed by almost the same procedure as before except that gauge tadpoles do not exist. Here we denote only graphs(Fig.25-31) contributing to the generating functional:

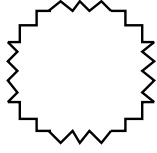


Fig.25

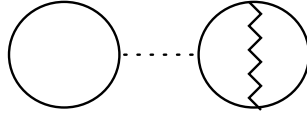


Fig.26

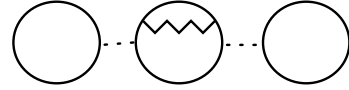


Fig.27

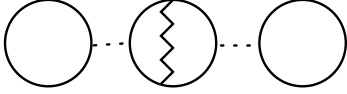


Fig.28

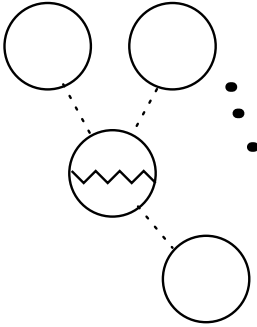


Fig.29

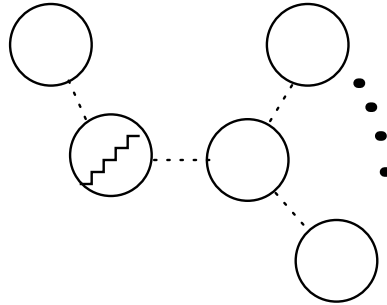


Fig.30

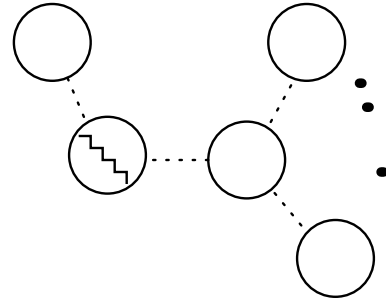


Fig.31

In order to calculate these graphs, we need Fig.32 which is obtained by differentiating the vacuum polarization tensor:

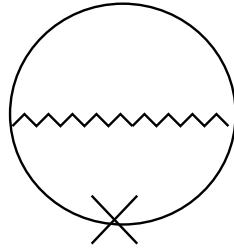


Fig.32

Namely,

$$\text{Fig.32} = -A_1 J - A_2 J^{D-1} + O(J^3) , \quad (56)$$

$$A_1 = \frac{2\alpha(D-1)f_2\Lambda^{D-2}}{(D-2)f_0} \left[1 - \frac{1}{g_V} \log(1 + g_V) \right] , \quad (57)$$

$$A_2 = \frac{\alpha D(D-1)f_D}{(D-2)f_0} \log(1+g_V) , \quad (58)$$

where $g_V \equiv -f_0 \Lambda^{D-2} G_V$ is the dimensionless Thirring coupling constant.

In the end of lengthy calculation, we found all graphs(Fig.6-8 and Fig.18-31) contributing to the generating functional $W[J]$ in the next-to-leading order of $1/N$ expansion. By calculating all these graphs, we finally obtain $W[J]$ as

$$\frac{1}{\Omega} W[J] = (\text{Fig.6}) + (\text{Fig.7}) + (\text{Fig.8}) + (\text{Fig.18}) + \cdots + (\text{Fig.31}) \quad (59)$$

$$= \frac{1}{2} K J^2 + \frac{1}{D} P J^D , \quad (60)$$

where K, P are given by

$$K = NK_0 + K_1 , \quad (61)$$

$$K_0 = \frac{c_0}{1-g} , \quad (62)$$

$$K_1 = -\frac{A_1 + B_1}{(1-g)^2} , \quad (63)$$

$$P = NP_0 + P_1 , \quad (64)$$

$$P_0 = \frac{-c_1}{D-1} \left(\frac{1}{1-g} \right)^D , \quad (65)$$

$$P_1 = \left\{ -A_2 - B_2 + \frac{c_1 D(A_1 + B_1)}{c_0(D-1)} \left(\frac{g}{1-g} \right) \right\} \left(\frac{1}{1-g} \right)^D . \quad (66)$$

5 Effective Potential by Inversion

The order parameter for the dynamical symmetry breaking, $\varphi(J)$, is given by differentiating (60) with respect to source J :

$$\varphi(J) = \langle \bar{\psi} \psi \rangle_J = \frac{1}{\Omega} \frac{\partial W}{\partial J} = KJ + PJ^{D-1} . \quad (67)$$

We here made use of inversion method[13] to obtain the effective potential instead of taking a Legendre transformation. By inverting (67), we obtain

$$J = K^{-1} \varphi - K^{-1} P J^{D-1} \quad (68)$$

$$= K^{-1} \varphi - P K^{-D} \varphi^{D-1} \quad (69)$$

$$= K^{-1} \varphi + Q \varphi^{D-1} . \quad (70)$$

K^{-1} is expanded in $1/N$ as

$$K^{-1} = \frac{1}{NK_0} \left(1 - \frac{K_1}{NK_0} \right) . \quad (71)$$

From the relation

$$J = \frac{\partial V}{\partial \varphi} , \quad (72)$$

the effective potential of $D(2 < D < 4)$ -dimensional Thirring-Gross-Neveu model can be obtained in the next-to-leading order of $1/N$ expansion:

$$V = \frac{1}{2} K^{-1} \varphi^2 + \frac{1}{D} Q \varphi^D . \quad (73)$$

Dynamical symmetry breaking occurs if the equation $J = \frac{\partial V}{\partial \varphi} = 0$ has a non-zero solution, $\varphi \neq 0$. It is realized when $K^{-1} < 0$, and the critical surface is given by $K^{-1} = 0$. Note that we calculate all graphs through vacuum polarization. Therefore our effective potential and all our conclusion has no gauge dependence[13].

6 Critical Line

K^{-1} is given in (71) reads

$$K^{-1} = \frac{1}{NK_0} \left(1 - \frac{K_1}{NK_0} \right) \quad (74)$$

$$= \frac{1-g}{Nc_0} \left\{ 1 + \frac{1-g}{Nc_0} \frac{(A_1 + B_1)}{(1-g)^2} \right\} \quad (75)$$

$$= \frac{1}{Nc_0} \left\{ 1 - g + \frac{A_1 + B_1}{Nc_0} \right\} . \quad (76)$$

Now, the critical coupling constants are given by the equation $K^{-1} = 0$ which defines a surface (g_c, g_{Vc}, N_c) in the parameter space (g, g_V, N) :

$$0 = 1 - g_c + \frac{(D-1)}{2N_c} \left[1 - \frac{1}{\tilde{g}_{sc}} \log(1 + \tilde{g}_{sc}) \right] - \frac{(D-1)^2(4-D)}{2N_c(D-2)} \left[1 - \frac{1}{g_{Vc}} \log(1 + g_{Vc}) \right] , \quad (77)$$

where \tilde{g}_{sc} was defined in (52). We can see from (77) that $g_c \sim 1$ for large N_c , and therefore we can approximate this equation as

$$g_c \simeq 1 + \frac{D-1}{2N_c} - \frac{(D-1)^2(4-D)}{2N_c(D-2)} \left[1 - \frac{1}{g_{Vc}} \log(1 + g_{Vc}) \right] + O\left(\frac{1}{N_c^2} \log N_c \right) . \quad (78)$$

Eq.(78) works well when N is sufficiently large. We will investigate the structure of the critical surface using eq.(78).

Before investigating (78) in detail, we consider the pure Gross-Neveu model. Taking $g_{V_c} = 0$ in the eq.(78), the critical line of the dynamical symmetry breaking in the Gross-Neveu model is given by

$$g_c \simeq 1 + \frac{D-1}{2N_c} + O\left(\frac{1}{N_c^2} \log N_c\right). \quad (79)$$

It is remarkable that this critical line is exactly the same line obtained by using SD equation up to the next-to-leading order of $1/N$ expansion[16].

Let us return to (78) to look into the critical surface of Thirring-Gross-Neveu model. We consider here $D = 3$ for convenience. Then the critical line is written as

$$g_c = 1 + \frac{1 - 2H(g_{V_c})}{N_c}, \quad (80)$$

where $H(z)$ is defined by

$$H(z) \equiv 1 - \frac{1}{z} \log(1+z). \quad (81)$$

$H(z)$ is monotonically increasing function and $H(0) = 0, H(\infty) = 1$. Since $0 \leq H \leq 1$ and $N \geq 1$, we find $g_c < 2$ in (80). The critical line in the (g_V, N) plane is given in FIG.A-1 and FIG.A-2 for various values of g .

We here divide the region $0 < g < 2$ into three regions, (1) $g > 2$, (2) $0 < g < 1$ (FIG.A-1) and (3) $1 < g < 2$ (FIG.A-2), where $g = 1$ is the value of critical coupling constant at the leading order of the Gross-Neveu model. The forms of critical line in these region are different from each other as follows:

(1) $g > 2$

In this case, the chiral symmetry is always broken irrespectively of g_V and N .

(2) $1 < g < 2$ (FIG.A-1)

In this region, the critical line (80) reads

$$N_c = \frac{1 - 2H(g_{V_c})}{g_c - 1} < \frac{1}{g_c - 1}. \quad (82)$$

For $g > 1$, g_{V_c} can take a value which satisfy the equation $2H(g_{V_c}) < 1$. The critical line exists only in the region $N \leq \frac{1}{g_c - 1}$ and N_c decreases as g_{V_c} increases as shown in FIG.A-1.

The symmetry is dynamically broken when $N > \frac{1}{g_c - 1}$.

(3) $0 < g < 1$ (FIG.A-2)

In this case, N_c increases according to increasing g_{Vc} and there exists a critical value of N_c :

$$N_c = \frac{2H(g_{Vc}) - 1}{1 - g_c} < N_c(g_c, g_{Vc} = \infty) = \frac{1}{1 - g_c} . \quad (83)$$

The dynamical symmetry breaking does not occur when $N > N_c(g_c, \infty)$. This critical line is quite similar to the critical line obtained in the Thirring model [10][11]. Thirring interaction strongly affect the system in this region, $0 < g < 1$. Thus, the property of the critical line is drastically changed at $g = 1$.

This can be understood naturally as follows. $g = 1$ is the critical coupling constant of the Gross-Neveu model at the leading order of $1/N$ expansion, and Thirring interaction does not strongly affect the leading order. Therefore, for $g > 1$, Gross-Neveu interaction is dominant. The system behaves like the Gross-Neveu model, and the symmetry is broken almost all the region. As N increases, the effect of $1/N$ next-to-leading order becomes small, and the system is dominated by the tadpole of the leading order. Therefore the dynamical symmetry breaking occur in large N region for $g > 1$.

On the other hand, the critical behavior is quite different in $0 < g < 1$. In this region, the Thirring interaction strongly affects the system, and the system (or the critical line) becomes Thirring-like. There exists a critical value for N , $N_c(g_c, g_{Vc} = \infty) < \infty$. The dynamical symmetry breaking does not occur in the large N region, $N > N_c(g_{Vc} = \infty, g_c)$, even if $g_V \rightarrow \infty$. The symmetry is broken in the small N region. This is in contrast to the case $1 < g < 2$ where the system behaves like Gross-Neveu model.

Thus the critical behavior drastically changes at $g = 1$. The system behaves like Thirring model in $g < 1$, whereas it does like Gross-Neveu model in $g > 1$.

7 Conclusion and Discussion

In this paper, we have constructed the effective potential for the order parameter of the chiral symmetry, the fermion condensate $\langle \bar{\psi}\psi \rangle$ in the hybrid model of the Gross Neveu model and the Thirring model in $D(2 < D < 4)$ dimensions. From this potential, we

have shown existence of the chiral symmetry breaking and explicitly obtained the critical surface.

We have analysed our model using the inversion method in $1/N$ expansion. In this model, existence of Gross-Neveu interaction make our analysis complicated. So many diagrams contribute to the generating functional. But we found we do not have to calculate all the diagrams. We have expanded the generating functional $W[J]$ in terms of the infinitesimal source J , and estimate it on the order $O(J^D)$. In section4, we investigated systematically the order of diagrams with respect to source J , and determine which diagram contributes to the generating functional $W[J]$ or effective potential $V(\langle\bar{\psi}\psi\rangle)$. Resultant effective potential has no gauge dependence, because we calculated all diagrams through vacuum polarization.

From this effective potential, we obtained explicitly the critical surface which separates symmetric phase and broken phase of the chiral symmetry. Especially, if we consider the special case $g_V = 0$ (Gross-Neveu model), our result(79) reproduces exactly the same result obtained by using SD equation[16].

Kim et al.[15] have already studied Thirring Gross-Neveu model by using SD equation and they found critical surface. Although the original Lagrangian(2) has no gauge symmetry, they pretended the auxiliary massive vector field as really a gauge field without introducing hidden local symmetry. Furthermore, the SD equation becomes coupled integral equations for $A(p)$ and $B(p)$ in the full fermion propagator $S(p)^{-1} = \not{p}A(p) - B(p)$, which are difficult to solve. Therefore additional approximations (or assumptions) besides $1/N$ expansion were made in their analysis. They assumed that the form of $A(p)$ can be determine by using perturbation, and mass function $B(p)$ can be regarded as a constant. As a result of such an approximation, the effects of the next-to-leading order of the Gross-Neveu interaction were not included.

On the other hand, we succeeded in obtaining the effective potential and the critical line without using additional approximation besides $1/N$ expansion.

Acknowledgments

The author would like to thank Prof. K. Yamawaki, and Drs. T. Itoh and M. Sugiura

for valuable discussion and comments.

References

- [1] Y. Nambu and G. Jona-Lasinio, Phys. Rev. **122** (1961) 345.
- [2] T. Maskawa and H. Nakajima, Prog. Theor. Phys. **52** (1974) 1326;
R. Fukuda and T. Kugo, Nucl. Phys. **B117** (1976) 250;
V. A. Miransky, Nuovo. Cim. **90A** (1985) 149.
- [3] K.-I. Kondo, M. Tanabashi and K. Yamawaki, Mod. Phys. Lett. **A8** (1993) 2859;
Prog. Theor. Phys. **89** (1993) 1249.
- [4] K.-I. Kondo, H. Mino, and K. Yamawaki, Phys. Rev. **D39** (1989) 2430.
- [5] *Dynamical Symmetry Breaking*, ed. K. Yamawaki (World Scientific, 1991)
B. Holdom, Phys. Lett. **B150** (1985) 301;
K. Yamawaki, M. Bando and K. Matumoto, Phys. Rev. Lett. **56** (1986) 1335;
T. Akiba and T. Yanagida, Phys. Lett. **B169** (1986) 432;
T. Appelquist, D. Karabali and L. C. R. Wijewardhana, Phys. Rev. Lett. **57** (1986) 957.
- [6] V. A. Miransky, M. Tanabashi and K. Yamawaki, Phys. Lett. **B221** (1988) 177; Mod.
Phys. Lett. **A4** (1989) 1043;
Y. Nambu, Chicago Preprint EFI-89-08 (1989);
W. A. Bardeen, C. T. Hill and M. Lindner, Phys. Rev. Lett. **62** (1990) 1647.
- [7] D. J. Gross and A. Neveu, Phys. Rev. **D10** (1974) 3235;
B. Rosenstein, B. J. Warr and S. H. Park, Phys. Rep. **205** (1991) 59;
Y. Kikukawa and K. Yamawaki, Phys. Lett. **A9** (1994) 1183.
- [8] W. Thirring, Ann. of Phys. **3** (1958) 91.

- [9] D. K. Hong and S. H. Park, Phys. Rev. **D49** (1994) 5507;
M. Gomes, R. S. Mendes, R. F. Ribeiro and A. J. da Silva, Phys. Rev. **D43** (1991) 3516.
- [10] T. Itoh, Y. Kim, M. Sugiura and K. Yamawaki, Prog. Theor. Phys. **93** (1995) 417.
- [11] K.-I. Kondo, Nucl. Phys. **B** 450 (1995) 251.
- [12] M. Bando, T. Kugo and K. Yamawaki, Phys. Rep. **164** (1988) 217.
- [13] R. Fukuda, Phys. Rev. Lett. **61** (1988) 1549;
M. Ukita, M. Komachiya and R. Fukuda, Int. J. Mod. Phys. **A5** (1990) 1789;
R. Fukuda, “Novel use of the effective action”, in Dynamical Symmetry Breaking,
ed. K. Yamawaki (World Scientific, 1992).
- [14] C. Itzykson and J.- B. Zuber, Quantum Field Theory (McGraw-Hill, 1980);
S. Hands, hep-th/9411016.
- [15] T. Kim, W. Kye and J. Kim, hep-th/9509068; Phys. Rev. **D52** (1995) 6109.
- [16] S. Hands, A. Kocic and J. B. Kogut, Phys. Lett. **B** **273** (1991) 111;
H. He, Y. Kuang, Q. Wang, and Y. Yi, Phys. Rev. **D45** (1992) 4610.
- [17] J. M. Cornwall, R. Jackiw and E. Tomboulis, Phys. Rev. **D10** (1974) 2428.
- [18] K.-I. Kondo, Mod. Phys. Lett. **A8** (1993) 3031.

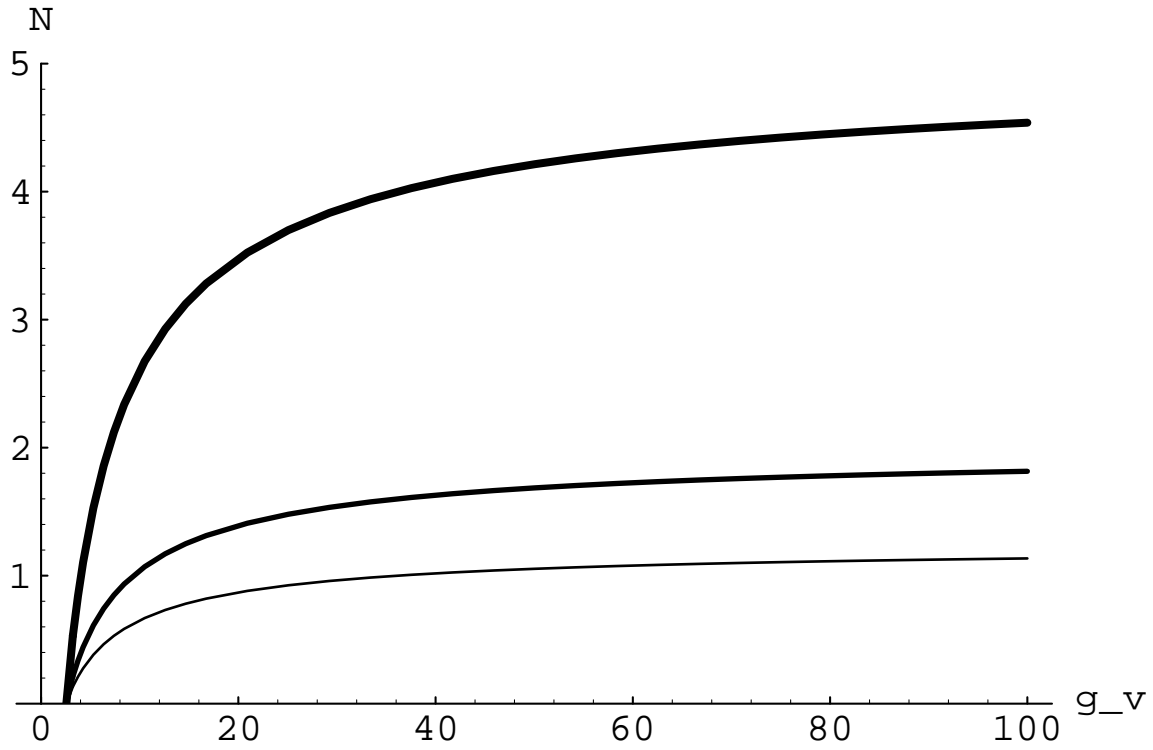


Fig.A-1:

The critical lines for various values of Gross-Neveu coupling constant g , ($g = 0.2$: lower line), ($g = 0.5$: middle line), ($g = 0.8$: upper line). Horizontal line and vertical line denote g_V and N , respectively.

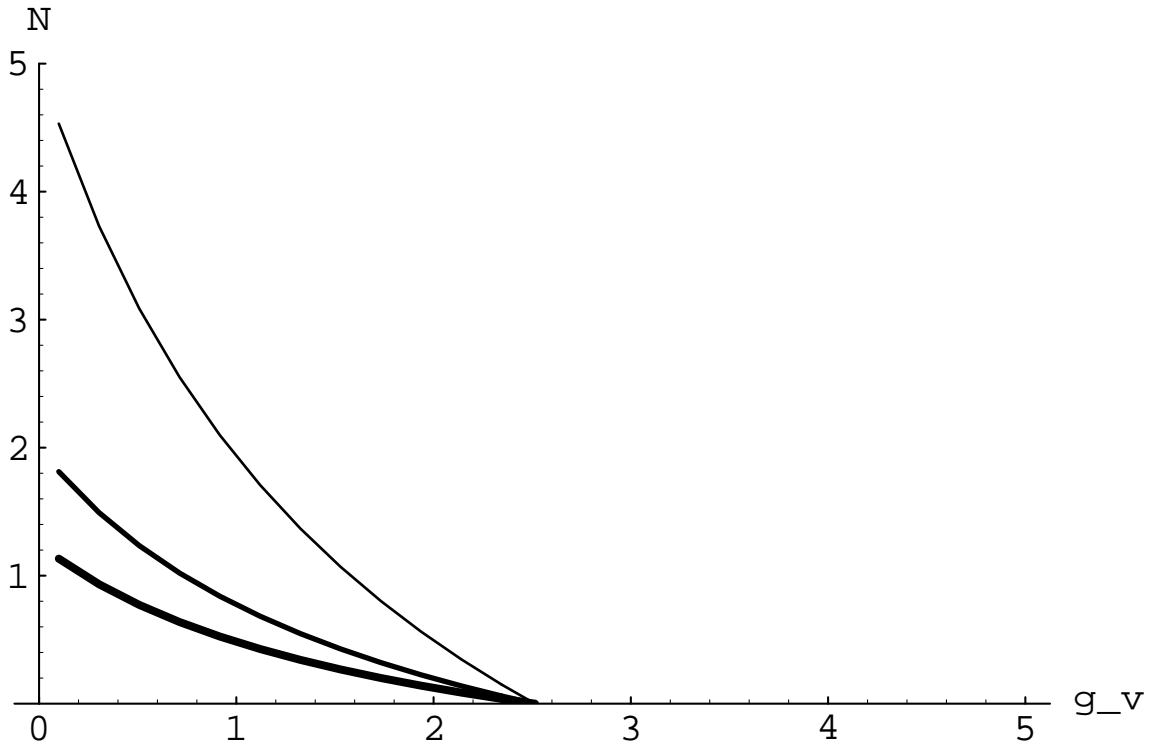


Fig.A-2

The critical lines for various values of Gross-Neveu coupling constant g , ($g = 1.2$: upper line), ($g = 1.5$: middle line), ($g = 1.8$: lower line). Horizontal line and vertical line denote g_V and N , respectively.